IL NUOVO CIMENTO Vol. 35 C, N. 6 Novembre-Dicembre 2012
DOI 10.1393/ncc/i2012-11370-x

Colloquia: LaThuile12

Bottomonium states

P. Krokovny for the Belle Collaboration
Budker Institute of Nuclear Physics SB RAS - Novosibirsk, Russia

ricevuto il 7 Settembre 2012

Summary. — Recent results on studies of bottomonium states at Belle are reported. The results are obtained with a 121.4 fb^{-1} data sample collected with the Belle detector in the vicinity of the $\Upsilon(5S)$ resonance at the KEKB asymmetric-energy e^+e^- collider.

PACS 14.40.-n – Mesons.

1. – Introduction

Bottomonium is the bound system of $b\bar{b}$ quarks and is considered an excellent laboratory to study Quantum Chromodynamics (QCD) at low energies. The system is approximately non-relativistic due to the large b quark mass, and therefore the quark-antiquark QCD potential can be investigated via $b\bar{b}$ spectroscopy.

The spin-singlet states $h_b(mP)$ and $\eta_b(nS)$ alone provide information concerning the spin-spin (or hyperfine) interaction in bottomonium. Measurements of the $h_b(mP)$ masses provide unique access to the P-wave hyperfine splitting, the difference between the spin-weighted average mass of the P-wave triplet states ($\chi_{bJ}(nP)$ or n^3P_J) and that of the corresponding $h_b(mP)$, or n^1P_1. These splittings are predicted to be close to zero [1], and recent measurements of the $h_c(1P)$ mass validates this expectation for charmonium.

Recently, the CLEO Collaboration observed the process $e^+e^- \to h_c(1P)\pi^+\pi^-$ at a rate comparable to that for $e^+e^- \to J/\psi\pi^+\pi^-$ in data taken above open charm threshold [2]. Such a large rate was unexpected because the production of $h_c(1P)$ requires a c-quark spin-flip, while production of J/ψ does not. Similarly, the Belle Collaboration observed anomalously high rates for $e^+e^- \to \Upsilon(nS)\pi^+\pi^-$ $(n = 1, 2, 3)$ at energies near the $\Upsilon(5S)$ mass [3]. Together, these observations motivated a more detailed study of bottomonium production at the $\Upsilon(5S)$ resonance.

We use a 121.4 fb^{-1}data sample collected on or near the peak of the $\Upsilon(5S)$ resonance ($\sqrt{s} \sim 10.865$ GeV) with the Belle detector [4] at the KEKB asymmetric energy e^+e^- collider [5].

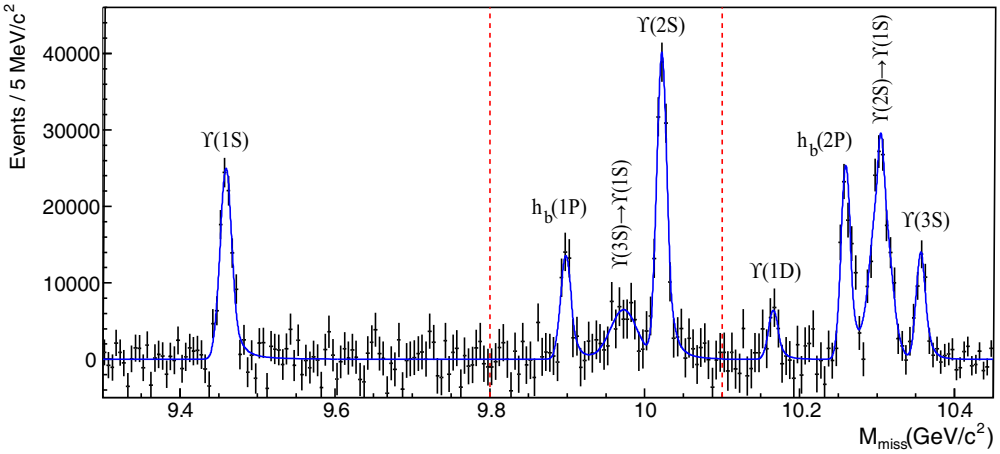

Fig. 1. – The inclusive $M_{\rm miss}(\pi^+\pi^-)$ spectrum with the combinatorial background and K^0_S contribution subtracted (points with errors) and signal component of the fit function overlaid (smooth curve). The vertical lines indicate boundaries of the fit regions.

2. – Observation of $h_b(mP)$

Our hadronic event selection requires a reconstructed primary vertex consistent with the run-averaged interaction point, at least three high-quality charged tracks. The $\pi^+\pi^-$ candidates are pairs of well reconstructed, oppositely charged tracks that are identified as pions and are not consistent with being electrons. Continuum $e^+e^- \to q\bar{q}$ $(q = u, d, s, c)$ background is suppressed by requiring the ratio of the second to zeroth Fox-Wolfram moments to satisfy $R_2 < 0.3$. More details can be found in ref. [6].

For all the $\pi^+\pi^-$ combinations we calculate missing mass defined as $M_{\rm miss}(\pi^+\pi^-) \equiv \sqrt{(P_{\Upsilon(5S)} - P_{\pi^+\pi^-})^2}$, where $P_{\Upsilon(5S)}$ is the 4-momentum of the $\Upsilon(5S)$ determined from the beam momenta and $P_{\pi^+\pi^-}$ is the 4-momentum of the $\pi^+\pi^-$ system. The $M_{\rm miss}(\pi^+\pi^-)$ spectrum is divided into three adjacent regions with boundaries at $M_{\rm miss}(\pi^+\pi^-) = 9.3$, 9.8, 10.1 and 10.45 GeV/c^2 and fitted separately in each region. In the third region, prior to fitting, we perform bin-by-bin subtraction of the background associated with the $K^0_S \to \pi^+\pi^-$ production. To fit the combinatorial background we use a 6th-7th order Chebyshev polynomial function for the first two (third) regions. The signal component of the fit includes all signals observed in the $\mu^+\mu^-\pi^+\pi^-$ data as well as those arising from $\pi^+\pi^-$ transitions to $h_b(mP)$ and $\Upsilon(1D)$. The peak positions of all signals are floated, except that for $\Upsilon(3S) \to \Upsilon(1S)\pi^+\pi^-$, which is poorly constrained by the fit. The $M_{\rm miss}(\pi^+\pi^-)$ spectrum, after subtraction of all the background contributions along with the signal component of the fit function overlaid is shown in fig. 1, where clear signals of both $h_b(1P)$ and $h_b(2P)$ are visible. The signal parameters are listed in table I. Statistical significance of all signals except that for the $\Upsilon(1D)$ exceeds 5σ.

The measured masses of $h_b(1P)$ and $h_b(2P)$ are $M = (9898.3 \pm 1.1^{+1.0}_{-1.1})\,{\rm MeV}/c^2$ and $M = (10259.8 \pm 0.6^{+1.4}_{-1.0})\,{\rm MeV}/c^2$, respectively. Using the world average masses of the $\chi_{bJ}(nP)$ states, we determine the hyperfine splittings to be $\Delta M_{\rm HF} = (+1.6 \pm 1.5)\,{\rm MeV}/c^2$ and $(+0.5^{+1.6}_{-1.2})\,{\rm MeV}/c^2$, respectively, where statistical and systematic uncertainties are combined in quadrature.

TABLE I. – *The yield and mass determined from the fits to the* $M_{\rm miss}(\pi^+\pi^-)$ *distributions.*

	Yield, 10^3	Mass, MeV/c^2
$\Upsilon(1S)$	$105.2 \pm 5.8 \pm 3.0$	$9459.4 \pm 0.5 \pm 1.0$
$h_b(1P)$	$50.4 \pm 7.8^{+4.5}_{-9.1}$	$9898.3 \pm 1.1^{+1.0}_{-1.1}$
$3S \to 1S$	56 ± 19	9973.01
$\Upsilon(2S)$	$143.5 \pm 8.7 \pm 6.8$	$10022.3 \pm 0.4 \pm 1.0$
$\Upsilon(1D)$	22.0 ± 7.8	10166.2 ± 2.6
$h_b(2P)$	$84.4 \pm 6.8^{+23.}_{-10.}$	$10259.8 \pm 0.6^{+1.4}_{-1.0}$
$2S \to 1S$	$151.7 \pm 9.7^{+9.0}_{-20.}$	$10304.6 \pm 0.6 \pm 1.0$
$\Upsilon(3S)$	$45.6 \pm 5.2 \pm 5.1$	$10356.7 \pm 0.9 \pm 1.1$

We also measure the ratio of cross sections $R \equiv \frac{\sigma(h_b(mP)\pi^+\pi^-)}{\sigma(\Upsilon(2S)\pi^+\pi^-)}$. To determine the reconstruction efficiency we use the results of resonant structure studies reported below. We determine the ratio of cross sections to be $R = 0.46 \pm 0.08^{+0.07}_{-0.12}$ for the $h_b(1P)$ and $R = 0.77 \pm 0.08^{+0.22}_{-0.17}$ for the $h_b(2P)$. Hence $\Upsilon(5S) \to h_b(mP)\pi^+\pi^-$ and $\Upsilon(5S) \to \Upsilon(2S)\pi^+\pi^-$ proceed at similar rates, despite the fact that the production of $h_b(mP)$ requires a spin-flip of a b-quark.

3. – Observation of $Z_b(10610)$ and $Z_b(10650)$

As it was mentioned above, the processes $\Upsilon(5S) \to h_b(mP)\pi^+\pi^-$, which require a heavy-quark spin flip, are found to have rates that are comparable to those for the heavy-quark spin conserving transitions $\Upsilon(5S) \to \Upsilon(nS)\pi^+\pi^-$, where $n = 1, 2, 3$. These observations differ from *a priori* theoretical expectations and strongly suggest that some exotic mechanisms are contributing to $\Upsilon(5S)$ decays.

First we perform an amplitude analysis of three-body $\Upsilon(5S) \to \Upsilon(nS)\pi^+\pi^-$ decays. To reconstruct $\Upsilon(5S) \to \Upsilon(nS)\pi^+\pi^-$, $\Upsilon(nS) \to \mu^+\mu^-$ candidates we select events with four charged tracks with zero net charge that are consistent with coming from the interaction point. Charged pion and muon candidates are required to be positively identified. Exclusively reconstructed events are selected by the requirement $|M_{\rm miss}(\pi^+\pi^-) - M(\mu^+\mu^-)| < 0.2\,{\rm GeV}/c^2$. Candidate $\Upsilon(5S) \to \Upsilon(nS)\pi^+\pi^-$ events are selected by requiring $|M_{\rm miss}(\pi^+\pi^-) - m_{\Upsilon(nS)}| < 0.05\,{\rm GeV}/c^2$, where $m_{\Upsilon(nS)}$ is the mass of an $\Upsilon(nS)$ state [8]. Sideband regions are defined as $0.05\,{\rm GeV}/c^2 < |M_{\rm miss}(\pi^+\pi^-) - m_{\Upsilon(nS)}| < 0.10\,{\rm GeV}/c^2$. To remove background due to photon conversions in the innermost parts of the Belle detector we require $M^2(\pi^+\pi^-) > 0.20/0.14/0.10\,{\rm GeV}/c^2$ for a final state with an $\Upsilon(1S), \Upsilon(2S), \Upsilon(3S)$, respectively. More details can be found in ref. [7].

Amplitude analyses are performed by means of unbinned maximum-likelihood fits to two-dimensional $M^2[\Upsilon(nS)\pi^+]$ *vs.* $M^2[\Upsilon(nS)\pi^-]$ Dalitz distributions. The fractions of signal events in the signal region are determined from fits to the $M_{\rm miss}(\pi^+\pi^-)$ spectrum and are found to be 0.937 ± 0.015(stat.), 0.940 ± 0.007(stat.), 0.918 ± 0.010(stat.) for final states with $\Upsilon(1S)$, $\Upsilon(2S)$, $\Upsilon(3S)$, respectively. The variation of reconstruction efficiency across the Dalitz plot is determined from a GEANT-based MC simulation. The distribution of background events is determined using sideband events and found to be uniform across the Dalitz plot.

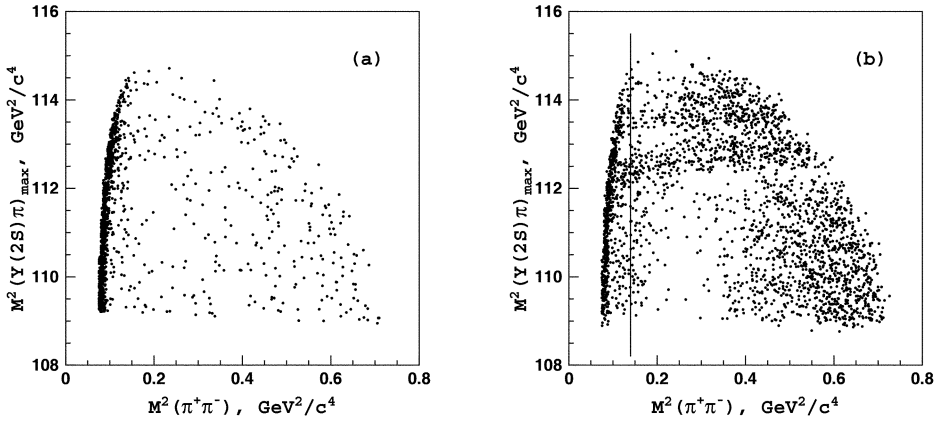

Fig. 2. – Dalitz plots for $\Upsilon(2S)\pi^+\pi^-$ events in the (a) $\Upsilon(2S)$ sidebands; (b) $\Upsilon(2S)$ signal region. Events to the left of the vertical line are excluded.

Dalitz distributions of events in the $\Upsilon(2S)$ sidebands and signal regions are shown in figs. 2(a) and 2(b), respectively, where $M(\Upsilon(nS)\pi)_{\rm max}$ is the maximum invariant mass of the two $\Upsilon(nS)\pi$ combinations. Two horizontal bands are evident in the $\Upsilon(2S)\pi$ system near $112.6\,\mathrm{GeV}^2/c^4$ and $113.3\,\mathrm{GeV}^2/c^4$, where the distortion from straight lines is due to interference with other intermediate states, as demonstrated below. One-dimensional invariant-mass projections for events in the $\Upsilon(nS)$ signal regions are shown in fig. 3, where two peaks are observed in the $\Upsilon(nS)\pi$ system near $10.61\,\mathrm{GeV}/c^2$ and $10.65\,\mathrm{GeV}/c^2$. In the following we refer to these structures as $Z_b(10610)$ and $Z_b(10650)$, respectively.

We parametrize the $\Upsilon(5S) \to \Upsilon(nS)\pi^+\pi^-$ three-body decay amplitude by

$$M = A_{Z_1} + A_{Z_2} + A_{f_0} + A_{f_2} + A_{\rm nr}, \tag{1}$$

where A_{Z_1} and A_{Z_2} are amplitudes to account for contributions from the $Z_b(10610)$ and $Z_b(10650)$, respectively. Here we assume that the dominant contributions come from amplitudes that preserve the orientation of the spin of the heavy quarkonium state and, thus, both pions in the cascade decay $\Upsilon(5S) \to Z_b\pi \to \Upsilon(nS)\pi^+\pi^-$ are emitted in an S-wave with respect to the heavy quarkonium system. An angular analysis support this assumption [9]. Consequently, we parametrize the observed $Z_b(10610)$ and $Z_b(10650)$ peaks with an S-wave Breit-Wigner function $BW(s, M, \Gamma) = \frac{\sqrt{M\Gamma}}{M^2-s-iM\Gamma}$, where we do not consider possible s-dependence of the resonance width. To account for the possibility of $\Upsilon(5S)$ decay to both $Z_b^+\pi^-$ and $Z_b^-\pi^+$, the amplitudes A_{Z_1} and A_{Z_2} are symmetrized with respect to π^+ and π^- transposition. Using isospin symmetry, the resulting amplitude is written as

$$A_{Z_k} = a_{Z_k} e^{i\delta_{Z_k}} (BW(s_1, M_k, \Gamma_k) + BW(s_2, M_k, \Gamma_k)), \tag{2}$$

where $s_1 = M^2[\Upsilon(nS)\pi^+]$, $s_2 = M^2[\Upsilon(nS)\pi^-]$. The relative amplitudes a_{Z_k}, phases δ_{Z_k}, masses M_k and widths Γ_k $(k = 1, 2)$ are free parameters. We also include the A_{f_0} and A_{f_2} amplitudes to account for possible contributions in the $\pi^+\pi^-$ channel from the $f_0(980)$ scalar and $f_2(1270)$ tensor states, respectively. We use a Breit-Wigner function

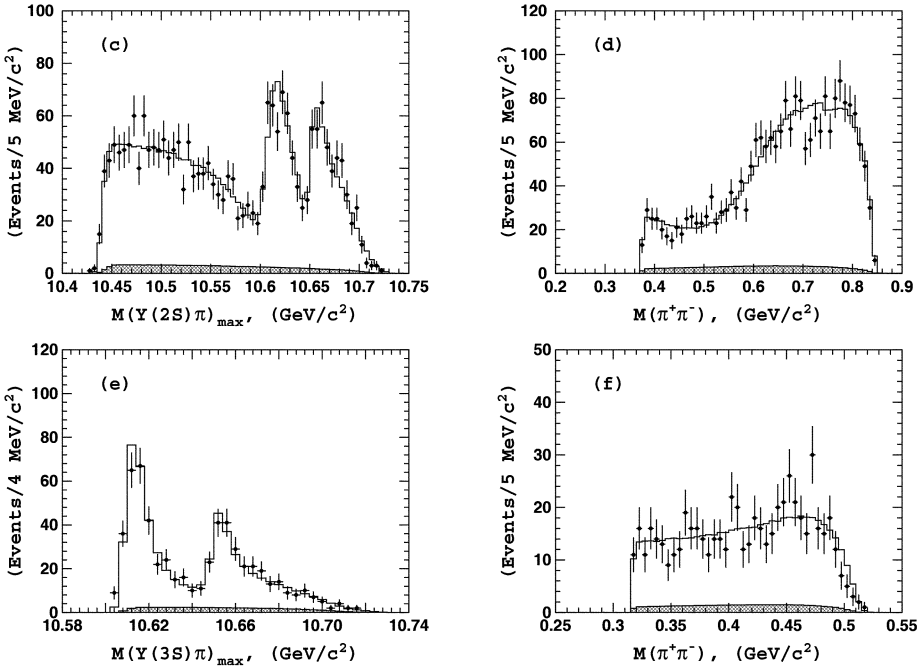

Fig. 3. – Comparison of fit results (open histogram) with experimental data (points with error bars) for events in the $\Upsilon(2S)$ (top) and $\Upsilon(3S)$ (bottom) signal regions. The hatched histogram shows the background component.

to parametrize the $f_2(1270)$ and a coupled-channel Breit-Wigner function for the $f_0(980)$. The mass and width of the $f_2(1270)$ state are fixed at their world average values [8]; the mass and the coupling constants of the $f_0(980)$ state are fixed at values determined from the analysis of $B^+ \to K^+\pi^+\pi^-$: $M[f_0(980)] = 950\,\mathrm{MeV}/c^2$, $g_{\pi\pi} = 0.23$, $g_{KK} = 0.73$ [10].

Following suggestions in ref. [11], the non-resonant amplitude $A_{\rm nr}$ is parametrized as $A_{\rm nr} = a_1^{\rm nr}\, e^{i\delta_1^{\rm nr}} + a_2^{\rm nr}\, e^{i\delta_2^{\rm nr}}\, s_3$, where $s_3 = M^2(\pi^+\pi^-)$ (s_3 is not an independent variable and can be expressed via s_1 and s_2 but we use it here for clarity), $a_1^{\rm nr}$, $a_2^{\rm nr}$, $\delta_1^{\rm nr}$ and $\delta_2^{\rm nr}$ are free parameters of the fit.

The logarithmic likelihood function $\mathcal{L}$ is then constructed as

$$\mathcal{L} = -2\sum \log(f_{\rm sig} S(s_1, s_2) + (1 - f_{\rm sig}) B(s_1, s_2)), \tag{3}$$

where $S(s_1, s_2)$ is the density of signal events $|M(s_1, s_2)|^2$ convolved with the detector resolution function, $B(s_1, s_2)$ describes the combinatorial background that is considered to be constant and $f_{\rm sig}$ is the fraction of signal events in the data sample. Both $S(s_1, s_2)$ and $B(s_1, s_2)$ are efficiency corrected.

Results of the fits to $\Upsilon(5S) \to \Upsilon(nS)\pi^+\pi^-$ signal events are shown in fig. 3, where one-dimensional projections of the data and fits are compared. The combined statistical significance of the two peaks exceeds $10\,\sigma$ for all tested models and for all $\Upsilon(nS)\pi^+\pi^-$ channels.

To study the resonant substructure of the $\Upsilon(5S) \to h_b(mP)\pi^+\pi^-$ ($m = 1, 2$) three-body decays we measure their yield as a function of the $h_b(1P)\pi^\pm$ invariant mass. The

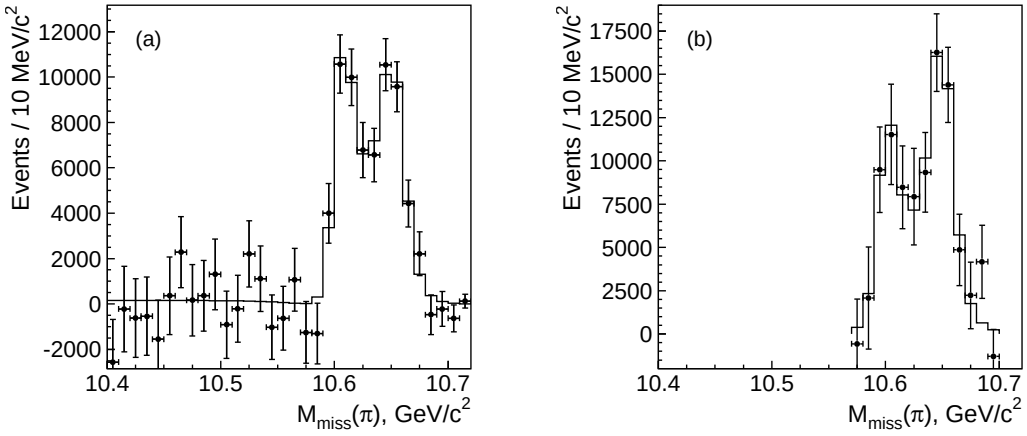

Fig. 4. – The (a) $h_b(1P)$ and (b) $h_b(2P)$ yields as a function of $M_{\rm miss}(\pi)$ (points with error bars) and results of the fit (histogram).

decays are reconstructed inclusively using missing mass of the $\pi^+\pi^-$ pair, $M_{\rm miss}(\pi^+\pi^-)$. We fit the $M_{\rm miss}(\pi^+\pi^-)$ spectra in bins of $h_b(1P)\pi^\pm$ invariant mass, defined as the missing mass of the opposite sign pion, $M_{\rm miss}(\pi^\mp)$. We combine the $M_{\rm miss}(\pi^+\pi^-)$ spectra for the corresponding $M_{\rm miss}(\pi^+)$ and $M_{\rm miss}(\pi^-)$ bins and we use half of the available $M_{\rm miss}(\pi)$ range to avoid double counting.

The fit function is a sum of peaking components due to dipion transitions and combinatorial background as described sect. **2**. The positions of all peaking components are fixed to the values measured from the fit to the overall $M(\pi^+\pi^-)$ spectrum (see table I).

Since the $\Upsilon(3S) \to \Upsilon(1S)$ reflection is not well constrained by the fits, we determine its normalization relative to the $\Upsilon(5S) \to \Upsilon(2S)$ signal from the exclusive $\mu^+\mu^-\pi^+\pi^-$ data for every $M_{\rm miss}(\pi)$ bin. In case of the $h_b(2P)$ we use the range of $M_{\rm miss}(\pi^+\pi^-) < 10.34\,{\rm GeV}/c^2$, to exclude the region of the $K^0_S \to \pi^+\pi^-$ reflection. The peaking components include the $\Upsilon(5S) \to h_b(2P)$ signal and a $\Upsilon(2S) \to \Upsilon(1S)$ reflection.

The results for the yield of $\Upsilon(5S) \to h_b(mP)\pi^+\pi^-$ $(m = 1, 2)$ decays as a function of the $M_{\rm miss}(\pi)$ are shown in fig. 4. The distribution for the $h_b(1P)$ exhibits a clear two-peak structure without a significant non-resonant contribution. The distribution for the $h_b(2P)$ is consistent with the above picture, though the available phase-space is much smaller. We associate the two peaks with the production of the $Z_b(10610)$ and $Z_b(10650)$. To fit the $M_{\rm miss}(\pi)$ spectrum we use the following combination:

$$|BW_1(s, M_1, \Gamma_1) + ae^{i\phi} BW_1(s, M_2, \Gamma_2) + be^{i\psi}|^2 \frac{qp}{\sqrt{s}}. \tag{4}$$

Here $\sqrt{s} \equiv M_{\rm miss}(\pi)$; the variables M_k, Γ_k $(k = 1, 2)$, a, ϕ, b and ψ are free parameters; $\frac{qp}{\sqrt{s}}$ is a phase-space factor, where p (q) is the momentum of the pion originating from the $\Upsilon(5S)$ (Z_b) decay measured in the rest frame of the corresponding mother particle. The P-wave Breit-Wigner amplitude is expressed as $BW_1(s, M, \Gamma) = \frac{\sqrt{M\,\Gamma}\,F\,(q/q_0)}{M^2 - s - iM\,\Gamma}$. Here F is the P-wave Blatt-Weisskopf form factor $F = \sqrt{\frac{1+(q_0R)^2}{1+(qR)^2}}$, q_0 is a daughter momentum calculated with pole mass of its mother, $R = 1.6\,{\rm GeV}^{-1}$. The function (eq. (4)) is

convolved with the detector resolution function, integrated over the histogram bin and corrected for the reconstruction efficiency. The fit results are shown as solid histograms in fig. 4. We find that the non-resonant contribution is consistent with zero in accord with the expectation that it is suppressed due to heavy quark spin-flip. In case of the $h_b(2P)$ we fix the non-resonant amplitude at zero.

4. – Conclusion

In summary, we have observed the P-wave spin-singlet bottomonium states $h_b(1P)$ and $h_b(2P)$ in the reaction $e^+e^- \to \Upsilon(5S) \to h_b(mP)\pi^+\pi^-$. The measured hyperfine splittings are consistent with zero as expected. A detailed analysis revealed that $h_b(mP)$ states in $\Upsilon(5S)$ decays are dominantly produced via intermediate charged bottomonium-like resonances $Z_b(10610)$ and $Z_b(10650)$. Resonances $Z_b(10610)$ and $Z_b(10650)$ have also been observed in decays $\Upsilon(5S) \to \Upsilon(nS)\pi^+\pi^-$. Weighted averages over all five channels give $M = 10607.2 \pm 2.0\,\mathrm{MeV}/c^2$, $\Gamma = 18.4 \pm 2.4\,\mathrm{MeV}$ for the $Z_b(10610)$ and $M = 10652.2 \pm 1.5\,\mathrm{MeV}/c^2$, $\Gamma = 11.5 \pm 2.2\,\mathrm{MeV}$ for the $Z_b(10650)$, where statistical and systematic errors are added in quadrature. The $Z_b(10610)$ production rate is similar to that of the $Z_b(10650)$ for each of the five decay channels. Their relative phase is consistent with zero for the final states with the $\Upsilon(nS)$ and consistent with 180 degrees for the final states with $h_b(mP)$. Analysis of charged pion angular distributions [9] favor the $J^P = 1^+$ spin-parity assignment for both the $Z_b(10610)$ and $Z_b(10650)$. Since the $\Upsilon(5S)$ has negative G-parity, the Z_b states have positive G-parity due to the emission of the pion.

The minimal quark content of the $Z_b(10610)$ and $Z_b(10650)$ is a four quark combination. The measured masses of these new states are a few MeV/c^2 above the thresholds for the open beauty channels $B^*\overline{B}$ ($10604.6\,\mathrm{MeV}/c^2$) and $B^*\overline{B}^*$ ($10650.2\,\mathrm{MeV}/c^2$). This suggests a "molecular" nature of these new states, which might explain most of their observed properties [12].

REFERENCES

[1] Godfrey S. and Rosner J. L., *Phys. Rev. D*, **66** (2002) 014012.
[2] Pedlar T. K. *et al.* (CLEO Collaboration), *Phys. Rev. Lett*, **107** (2011) 041803.
[3] Chen K.-F. *et al.* (Belle Collaboration), *Phys. Rev. Lett.*, **100** (2008) 112001.
[4] Abashian A. *et al.* (Belle Collaboration), *Nucl. Instrum. Methods Phys. Res. A*, **479** (2002) 117.
[5] Kurokawa S. and Kikutani E., *Nucl. Instrum. Methods Phys. Res. A*, **499** (2003) 1, and other papers included in these Proceedings.
[6] Adachi I. *et al.* (Belle Collaboration), *Phys. Rev. Lett.*, **108** (2012) 032001.
[7] Bondar A., Garmash A., Mizuk R., Santel D., Kinoshita K. *et al.* (Belle Collaboration), *Phys. Rev. Lett.*, **108** (2012) 122001.
[8] Nakamura K. *et al.* (Particle Data Group), *J. Phys. G*, **37** (2010) 075021.
[9] Adachi I. *et al.* (Belle Collaboration), arXiv:1105.4583 [hep-ex].
[10] Garmash A. *et al.* (Belle Collaboration), *Phys. Rev. Lett.*, **96** (2006) 251803.
[11] Voloshin M. B., *Prog. Part. Nucl. Phys.*, **61** (2008) 455; Voloshin M. B., *Phys. Rev. D*, **74** (2006) 054022 and references therein.
[12] Bondar A. E., Garmash A., Milstein A. I., Mizuk R. and Voloshin M. B., *Phys. Rev. D*, **84** (2011) 054010.